

<https://doi.org/10.1038/s43246-024-00646-6>

Accelerating solar-powered desalination deployment through transferable learning

Check for updates

Ruoqing Wang¹ & Wei He^{1,2}

Solar desalination offers a promising solution to the global water shortage, yet it is underutilized compared to traditional fossil fuel-driven methods. Past solar desalination research prioritized efficiency enhancement and cost reduction, overlooking critical knowledge gaps and specific needs for facilitating the technology's adoption. Here we apply lessons from the successful development of photovoltaics and lithium-ion batteries to enhance the solar desalination impact's on water scarcity. We analyze four decades of research, noting consistent cost decreases in key solar desalination technologies, alongside variable efficiency trends. Investigating cost reduction strategies in photovoltaics and batteries reveals opportunities to accelerate solar desalination uptake. Our findings reveal cost-saving potential through economies-of-scale and learning-by-doing particularly in system-level innovations, which could yield benefits already seen in the photovoltaics, batteries and some membrane materials but not yet in solar desalination systems. We also propose adopting standardized metrics to monitor consistent progress across different technologies but distinct learning curves tailored to application scenarios, promoting targeted advancements for widespread adoption.

Water scarcity is a serious problem we are facing nowadays. It is predicted that one third to nearly half of the global urban population will have inadequate water resources by 2025¹. 97.5% of the water on earth is seawater and saline aquifers, desalination technology is a solution that can convert salt water into freshwater to alleviate the water shortage.

Desalination technologies include membrane and thermal desalination processes. Reverse osmosis (RO) and electrodialysis (ED) are the two main types of membrane-based desalination that require electrical energy. Thermal desalination includes multistage flash distillation (MSF), multi-effect distillation (MED) and vapor compress (VC) which can be thermal or mechanical. Also, in recent years, some desalination technologies with lower energy demand are emerging and under the development stage, including membrane distillation (MD), capacitive deionization (CDI) and forward osmosis (FO). Due to the abundant solar energy source on earth and no carbon emission while exploiting it, solar desalination is a promising sustainable approach to address the world's water scarcity without significant carbon emissions. Solar desalination usually can be divided into direct methods, such as solar still, and indirect methods which use either PV or solar collectors to harvest the solar energy for desalination systems.

Despite solar desalination being applied in many regions, such as Middle East and North America, its global use is limited due to high costs. To improve solar desalination technologies, there are two common

pathways: efficiency-prioritized and cost-prioritized research. Efficiency and cost are two key factors that motivate the development of solar desalination technologies. Efficiency is a crucial technical metric that leads to the technical improvement of the solar desalination system, whereas cost is one of the most important factors influencing market development, deployment, and consumer adoption.

High efficiency reduces energy and raw material usage, which in turn reduces carbon emissions and improves sustainability. Even in solar desalination or other clean energy applications, improving efficiency can reduce the materials used, thus reducing embodied carbon emissions. A highly efficient solar desalination system also improves land use in various applications. The improved efficiencies in desalination processes are likely to lead to a reduction in water cost over the long term through the advancement of desalination technologies in practice. Besides efficiency improvements, various other factors such as the manufacture of materials, supply chains of solar and desalination components, land costs, system installation and maintenance, labor costs, and regulatory costs affect the water cost of a solar desalination plant and its competitiveness in the market. Therefore, reducing water costs of solar desalination while providing high quality of water is usually prioritized from the deployment perspective.

Previous review papers on solar desalination usually focus on a techno-economic review or an energy assessment review of a single solar

¹Department of Engineering, King's College London, London, UK. ²Department of Mechanical Engineering, Massachusetts Institute of Technology, Cambridge, USA. e-mail: wei.4.he@kcl.ac.uk

desalination technology² or category³ or providing pathways for solar thermal desalination⁴ or electrical desalination⁵. Most of these focus on technology development, prioritizing either efficiency and/or cost, but rarely do they examine the knowledge gaps and requirements that technology developers need to accelerate the deployment of technology and the market development of solar desalination. To address the gap, we have tracked the cost and efficiency trends of key solar desalination technologies from literature and commercial plant databases. Our focus is on desalination technologies including RO, MSF, MD, ED/EDR, and direct solar desalination, as classified in Fig. 1. These technologies represent two main types of solar desalination and are the most commonly installed worldwide, contributing to the global desalination capacity of 69%, 18%, 7%, and 2%, respectively⁶. Subsequently, we apply the learning curve concept to identify critical factors that influence solar desalination deployment. By drawing insights from other industries that had accomplished significant cost reductions and rapid market development, such as photovoltaics (PV) and lithium-ion batteries, our goal is to collect evidence and foster a discussion on accelerating the adoption of solar desalination to enhance global water security. To achieve this, we summarize cost metrics that are essential for formulating a learning curve for solar desalination. We also introduce efficiency metrics and highlight the importance of monitoring efficiency improvements, as these directly contribute to cost reduction. Such tracking can facilitate further technological and engineering innovations, which are crucial for achieving significant long-term cost reductions.

Cost trend of solar desalination in the literature and market database

The water cost is usually the most influential factor to determine the technology deployment. The total cost of water in a solar desalination system includes the capital cost and operational and maintenance (O&M) costs. The components of the total water cost are shown in Fig. 2. The water cost (\$/m³) is calculated by dividing the sum of annual capital and O&M by the average annual desalinated water production.

Based on the surveyed data of water costs of solar desalination (Fig. 3), the water costs of commercialized desalination plants show clearer reductions compared to the costs of desalination systems reported in the literature. This discrepancy may arise because the water production costs collected from the literature are based on various assumptions, technical and financial resources, and supply chains, which differ locally across sites. Different salinities influence the overall water cost^{7–9}. It scales roughly linearly with the total dissolved salt (TDS) value, ranging from approximately \$3.3/m³ for a TDS of 3000 mg/L to about \$7.8/m³ for seawater⁸. The interest rates to finance solar desalination projects vary significantly between regions, ranging from 12% in India in 2013 to 5% in the Middle East in 2019^{10,11}. Furthermore, the economic factors considered in cost assessments vary among studies. For example, some analyses include labor and land expenses in the total water production costs, whereas others concentrate exclusively on capital investment. Also, the consideration of brine disposal cost could also lead to cost difference. The location of a desalination

operation is a crucial determinant in identifying appropriate brine disposal options and assessing the resulting environmental impacts. For inland locations, the deep well injection is the commonly used brine disposal method and for coastal areas, the brine can be disposed into the sea¹². Despite these differences, an analysis of five key solar desalination technologies from 1980 to 2023 indicates a general decrease in water production costs, though there are some deviations from this main trend (Fig. 3).

It is observed that the costs associated with commercial RO plants, which are not solely powered by solar energy, are lower than those reported in literature for laboratory-scale operations that are PV-powered. This discrepancy can be attributed to the larger capacity of commercial plants in comparison to their laboratory-scale counterparts. This finding aligns with observations from both commercial solar thermal desalination systems and computational modeling studies¹³. It is important to note that our analysis does not account for inflation over the period under review, which could affect the interpretation of cost trends.

Different approaches in cost modeling over the past four decades have directly affected the reported costs. For the RO, the water production costs were relatively low (less than \$10/m³) in the early 1980s. This could be because those studies only considered the system's lifetime as 10 years and did not include battery replacement costs^{14,15}, whereas the majority of studies now consider a lifetime of 20–30 years.

Moreover, the decreased water cost of solar desalination systems is benefited from technical improvements in PV panels, solar collectors and membrane designs as well as the integrated processes and competition in the markets¹⁶. Solar PV experienced a rapid cost reduction during the last decades. With every doubling of cumulative capacity installation of PV modules, the cost dropped 20% approximately since 1970s^{17,18}.

The cost of desalinating brackish water has been reduced by more than 50% in the last two decades, despite the fluctuating costs of seawater desalination, highlighting the development differences across salinities (Fig. 3). Innovations in membrane technology, such as enhancements in reducing membrane fouling and extending membrane lifespan, have significantly impacted water costs. The reduction in RO costs is primarily due to the substantial decrease in membrane costs. Furthermore, it is anticipated that if the costs of the ion-exchange membrane in ED are reduced and membrane performance is enhanced, ED could become more economically advantageous than RO across the entire brackish water salinity spectrum¹⁹.

Membrane costs significantly impact the overall cost of water production, largely due to the membrane manufacturing process being in its relatively early stages. In 2018, the cost of water production using MD could reach up to \$85/m³, attributed to both the small capacity of the plants and the high cost of membranes, making it economically unviable²⁰. The use of hollow fiber membranes, priced at \$1500/m²—being the only commercially available compact MD membrane with a smaller footprint than other types—further exacerbates this issue. However, alternative membrane types such as spiral wound membranes, at \$108/m², and flat-sheet membranes, at \$410/m², are available at lower costs, potentially reducing water costs of MD systems²¹. Depending on different types of membranes, they all have different levels of fouling and scaling problems, and some of the membranes such as tubular membrane consumes relatively high energy consumption compared to other types of membranes²².

Besides individual components, the overall system design configuration also plays a crucial role in determining water production costs. Keeper et al.¹⁵ demonstrated that incorporating an energy recovery pump can significantly lower water production costs by approximately 50% compared to systems without one, especially when operating under constant speed battery mode. They further noted that variable speed systems without batteries offer a cost advantage of \$9.05/m³. Ajiwiguna et al. explored how the water demand profile and system configuration impact the water production cost of PV-RO systems^{23,24}. They found that scenarios with variable water demand require larger capacities for seasonal water storage tanks (SWST) or batteries, leading to higher production costs compared to constant demand scenarios. Their analysis also revealed that PV-RO systems equipped only with batteries have the highest water production costs. In contrast,

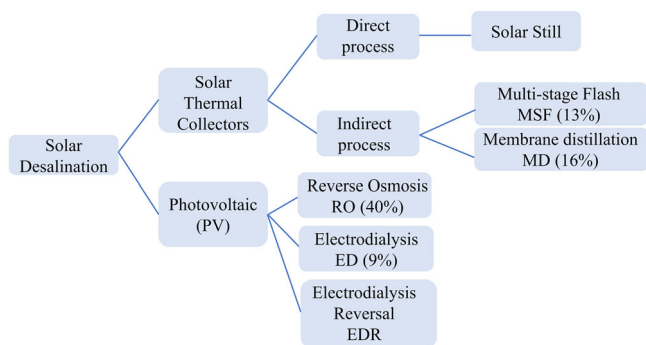


Fig. 1 | Classification of solar desalination. Solar desalination technologies are categorized into two main types: membrane-based methods (e.g., RO and ED) and thermal-based methods (e.g., MSF and MD).

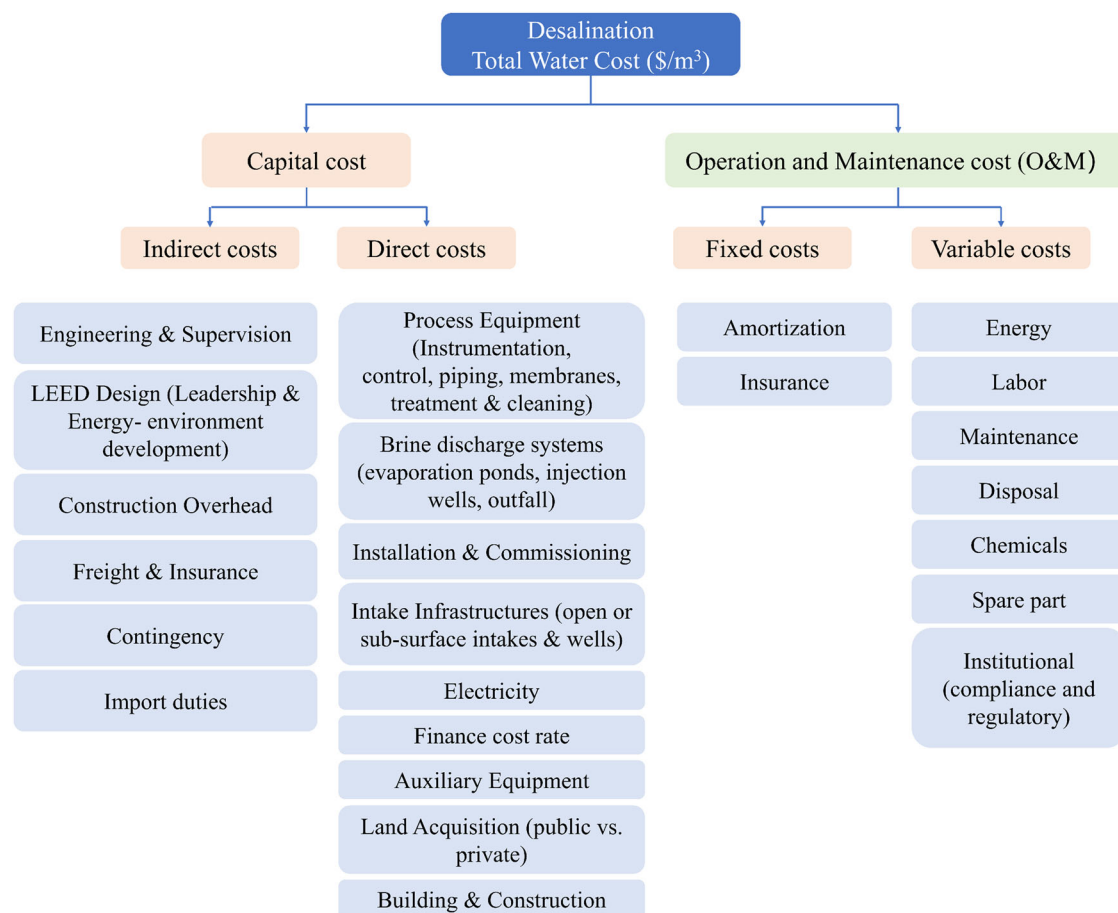


Fig. 2 | Breakdown of total water desalination costs. The total cost of desalination consists of two main components: capital costs (including both direct and indirect costs) and Operation and Maintenance costs (which are further divided into fixed and variable costs). Graph is redrawn and reprinted with permission from refs. 16,105,112,113.

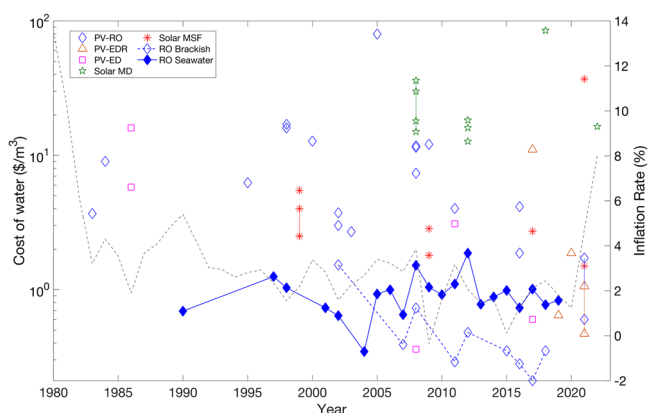


Fig. 3 | Water production cost of different solar desalination technologies from 1980 to 2023. The two points connected with solid line represents the range of water production cost in one study. Grey dash line is the inflation rate. Blue points with solid and dash line are the average cost of commercial RO plants (not solar-powered) for seawater and brackish water, respectively. Cost of water is calculated by dividing the sum of annual capital and O&M by the average annual desalinated water production. What needs to be noticed is that we did not consider the inflation rate into our cost data during the investigated period.

integrating SWST into PV-RO-Battery systems significantly reduces costs, with PV-RO systems using SWST alone offering the lowest costs in both variable and constant demand scenarios. To further optimize these design trade-offs, applying machine learning optimization algorithms, such as particle swarm optimization, can be effective. He et al. showed that

optimizing PV and EDR subsystems using this method reduced the levelized cost of water in the system by 45% to \$1.87/m³ and the capital cost by 34%, compared to traditionally designed and equivalently sized PV-EDR systems²⁵.

Efficiency trend of solar desalination in prior studies

Specific water productivity (SWP) is used in this study to compare the efficiency of the PV-powered and thermal-powered desalination systems. SWP is a key metric that represents the overall solar-to-water process of a solar thermal desalination system, and it is defined as the mass of water produced per solar radiation area per time²⁶. Because SWP incorporates both the environmental aspect and overall system performance, it is helpful when making techno-economic decisions²⁶. The equation and assumptions are shown in Section “Unified metric for solar desalination efficiency”. Figure 4 compares the specific energy consumption (SEC) and SWP among six solar desalination technologies, including the direct solar desalination. The SEC is inversely proportional to SWP due to the definition of the two terms. The SWP of indirect desalination technologies does not show an obvious rising trend during the 40 years. Whereas, the SWP of direct solar desalination increased rapidly in the last two decades.

Electrically-driven solar desalination

The SWP reviewed in this study ranges from 6.17 to 224.72 Lm⁻²h⁻¹, broader than Wang et al.’s study⁷. Here, the SEC varies broadly from 1.1–32.4 kWh/m³, while SEC in Wang et al.’s study was only from 2 to 4 kWh/m³ without considering much lower values for low salinity brackish water²⁷.

Unlike the SEC of PV-RO which shows a large variation in the past decades, the power consumption of commercial Seawater Desalination

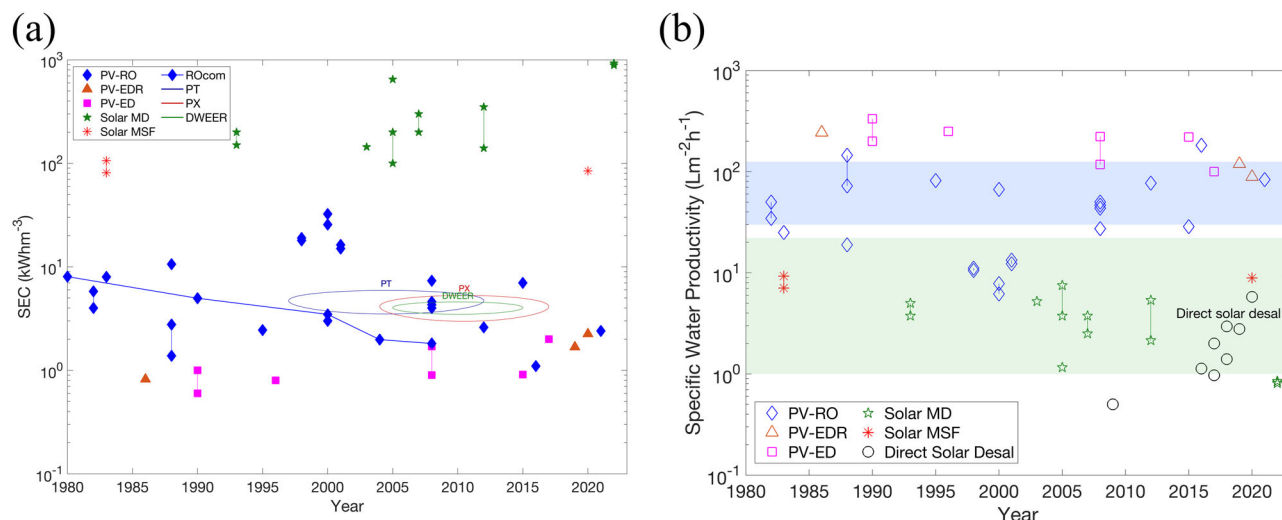


Fig. 4 | SEC and SWP comparison from 1980 to 2023. a SEC of different solar desalination technologies. Rocom: Commercial RO plants (not all powered by solar energy). Circles represent the SEC of RO using three types of energy recovery devices (ERDs). (PT: Pelton turbine, DWEER: dual work exchanger energy recovery, PX: pressure exchanger). **b** SWP of different desalination technologies. Two points

linked with a solid line represents the range of SWP in one study and here we assume the SWP of direct solar desalination equals its water production rate. (Blue dash line: the SWP range of PV-RO from Wang et al.'s study⁷; green dash line: the SWP range of STD from Wang et al.'s study⁷).

Reverse Osmosis (SWRO) (not all powered by solar energy) has decreased dramatically from approximately 16 kWh/m³ in 1970 to almost close to the theoretical minimum energy of 1.06 kWh/m³ in 2008 (Fig. 4a), which is attributed to the advanced high permeability membrane materials and innovations of ERDs and high-pressure pumps (HPPs)²⁸.

The theoretical minimum energy is the minimum energy used for pure water separation from seawater, which can help us understand how energy inputs can be used effectively through the desalination process and provide directions on how to reduce the SEC. The applied pressure equals to the osmotic pressure of seawater (Π_s) to force an infinitesimally small volume of water ($\bar{V}_w dn_w$) through a semipermeable membrane. It is independent of the desalination method²⁹ and can be expressed as²⁸:

$$-d(\Delta G_{mix}) = -RT \ln a_w dn_w = \Pi_s \bar{V}_w dn_w \quad (1)$$

where ΔG_{mix} denotes the free energy of mixing, R denotes the ideal gas constant, T denotes the absolute temperature, a_w and n_w denotes the activity of water and number of moles of water, respectively. Π_s denotes the osmotic pressure of the seawater and \bar{V}_w is the molar volume of water.

The SEC of SWRO decreased sharply over time because of the enhancement of ERDs (Fig. 3a). ERDs can recover some of the energy in the brine stream and relocate it to the feed stream using centrifugal or isobaric ERDs³⁰. In the early 90 s, the maximum energy recovery efficiency of Francis Turbines was 75%, which was first used in SWRO and lowered the SEC to 4–5 kWh/m³³¹. After 2000, isobaric pressure exchangers with an energy recovery efficiency of more than 96% replaced most centrifugal-driven ERDs³², further reducing power consumption for SWRO desalination to over 2 kWh/m³ at 50% recovery. However, due to the development of ERDs being almost saturated, it may play a minor role in the future reduction of SEC for RO.

HPPs are usually coupled with a variable frequency drive that can control the voltage and frequency applied to the motor, thus reducing unnecessary energy loss and reducing SEC when a larger variation of pressures is required for the plants³³. The efficiency of HPPs increases with the enlarging of their capacities³⁴. A large capacity of SWRO plant seems to be more effective in reducing the SEC of RO³⁰.

Enhancing the membrane permeability and membrane fouling can reduce the SEC of RO. Cohen-Tanugi et al.³⁵ demonstrated that the application of ultra-permeable membranes for SWRO and brackish water

RO allows a 15% and 46% of SEC reduction at the same permeate production per vessel, respectively. The RO process is constrained by thermodynamic principles, dictating that the applied pressure P_H cannot be reduced to lower than the osmotic pressure of the concentrate π_c . Consequently, within these thermodynamic limits, the potential for reducing SEC in RO is fundamentally constrained by the ability to enhance membrane permeability³⁶. So far, the SWRO plants are already working toward the thermodynamic limit as the P_H is only 10–20% higher than π_c .

Membrane fouling in RO is the microbes growing on the membrane surface, leading to an increase in SEC. To mitigate this phenomenon, modification of the membrane surface, such as coating the surface with PEG can be employed³⁷, despite meanwhile the membrane permeability is compromised. There is still room for the development of antifouling membranes in the future to reduce the energy demand for RO.

SEC fluctuations in PV-RO systems stem from studies primarily focusing on case studies across diverse locations, influenced by variations in feed water salinity and permeate water quality. Desalinating seawater requires more energy than desalinating brackish water, due to the higher salinity of seawater and, consequently, higher osmotic pressure than that of brackish water³⁸. This also applies to ED, which is favored at TDS < 2500 mg/L³⁹. More SEC is also consumed to improve the permeate water quality as an additional RO pass is required³⁰. Additionally, variations in system design, including system size, battery types, and the utilization of efficient HPPs and ERDs, result in differences in the SEC^{40,41}. From Fig. 4, some of the studies before 2000 have relatively lower SEC values that are within 4 kWh/m³. This could be due to the use of efficient HPPs and three-phase induction motor which require less energy consumption and produce more water compared with only using a DC motor^{42,43}.

Plant size universally affects the energy efficiency in solar desalination. The SEC of RO reaches the highest in 1998 in Fig. 4a because Herold et al. developed a PV-RO that has an approximately three times higher SEC (18–19 kWh/m³) than conventional medium to large size systems in Gran Canaria, which is due to the very small capacity (1 m³/d) of the plant and the involvement of the pre-treatment process⁴⁴. Later, Herold & Neskakis⁴⁵ developed a 0.8–3 m³/d capacity of PV-RO for seawater with SEC at 15 kWh/m³ and 16.3 kWh/m³, and the relatively higher SEC is because of the high feed pressure ranges from 45 bar to 63 bar. Typically, the working pressure of seawater for RO is lower than 85 bar, and the higher the feed pressure, the higher the energy consumption of the plant⁴⁶.

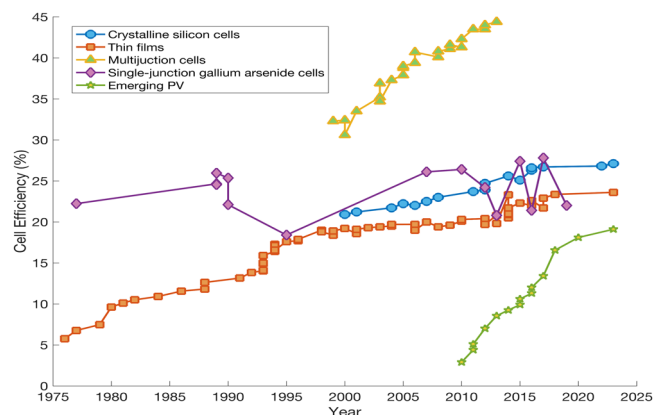


Fig. 5 | Best research cell efficiency progress. Five representative PV cells classified by different semiconductor materials are chosen to show the increasing trend of PV cell efficiency. Graph is redrawn from National Renewable Energy Laboratory (NREL) and the dataset of NREL's original can be found in Supplementary Data 1.

Furthermore, few studies focused on the efficiency improvement of PV-RO combination, instead, most studies would separate PV and RO, and improve their efficiency respectively⁴⁷. Ravel and Maiti⁴⁸ co-optimized the PV panel temperature and RO membrane hydrophilicity modification to reduce the SEC by 40%. Similarly, very few research on the efficiency improvement of PV-ED/EDR as a whole. However, studies show efficiency improvement in the ED/EDR system if considered separately. For example, batch ED operates under constant entropy generation or constant current enabling an improvement in energy consumption⁴⁹. Batch, semi-batch and stage RO processes can reduce SEC by over 25%, depending on the feed-water salinity⁵⁰. Also, the data we collected mostly came from site-specific PV-RO research where they focused more on whether their overall system performance can meet the local water requirement. Thus, the data is scattered and it is difficult to observe a successive efficiency improvement trend. PV-ED data collected could be insufficient and inconsistent, which may not represent the overall development.

PV efficiency

The efficiency of a variety of PV technologies was plotted from 1976 to the present (Fig. 5), showing an increasing trend for every category. The current highest research-cell efficiency is from Fraunhofer Institute for Solar Energy Systems (FhG-ISE), reaching 47.6%. Coupling solar energy with desalination systems can reduce the GHG emissions and environmental impacts, however, the steadily increasing research-cell efficiency does not contribute to the solar desalination efficiency improvement over the years, which raises the question of whether solar desalination is simply a combination of solar PV power generation and desalination for efficient solar-to-water conversion. Most of the highest efficiency PV cells are not massively manufactured yet, which is not available from the market and cannot be applied in the PV-RO/ED systems to improve the overall efficiency.

Also, the shown efficiencies in Fig. 5 are tested in standard testing conditions. In practice, the efficiency of solar PV varies with different operations and weather conditions⁵¹. The efficiency in winter is better than in summer and post-monsoon months in India from Vasisht et al.'s study⁵², which is due to the cool breezes and lower ambient temperatures resulting in intermittent natural cooling of the component surfaces. This leads to an important hurdle when integrated with desalination technologies as intermittent energy generation cannot provide stable water production. To overcome it and introduce flexibility into solar desalination, battery storage systems and water storage tanks are employed⁵³. The PV system in a battery-based system has a higher solar energy to electricity efficiency (8.8%) than a battery-less system (5.5%), whereas the SEC of both systems are relatively the same⁵⁴. Despite the battery-based system can provide larger annual water production and improve solar energy efficiency, the water cost of

battery-based system is higher than the battery-less system as the high battery cost and O&M cost, especially for small scale systems. There is also a trade-off between the water cost of solar desalination system and its efficiency. The use of water storage tanks to store excessive water instead of electricity in battery-less systems is likely more cost-competitive. Proper sizing and integration of solar PV fields, desalination plants and water storage tanks allow for more efficient use of excess solar irradiation so that smaller solar PV fields and larger desalination plants can adequately meet the load. The reduced size of solar PV fields also causes a significant economic improvement compared with battery-based systems without water storage tanks⁵⁵.

Solar thermal desalination (STD)

The SWP of STD systems reviewed in our study ranges from 0.81 to 9.26 $\text{Lm}^{-2}\text{h}^{-1}$, which aligns well with the range in Wang et al.'s study⁷. However, the available SEC of solar-powered MSF from the literature is very limited. MSF is a mature thermal desalination technology that has substantially optimized its efficiency by recovering the latent heat of evaporation effectively⁵⁶. The incorporation of external solar thermal collectors with MSF allows it to have high gained output ratios (GOR)⁵⁷. The SEC of MD and MSF covers a range of 100–926.8 kWh/m^3 and 81–106 kWh/m^3 , respectively. In comparison, SEC in Wang et al.'s study ranges from the best-performing MED systems which have 42 kWh/m^3 with a GOR of 15 to the STD without latent heat recovery that have 628 kWh/m^3 ^{3, 7, 58, 59}.

Nassrullah et al. compared the SEC of different MDs during the last few years, which has been significantly more variable from 1.24 kWh/m^3 for AGMD which utilized the natural temperature gradients of waste energy in 1983 to around 1 kWh/m^3 for AGMD in 2007, although they are not all powered by solar energy². The vast difference between different SEC of MD as shown in Fig. 4b is due to various operating conditions (such as feed water temperature, and feed water flow rate) and different MD system types. In the DCMD configuration, although high fluxes can be attained, the substantial heat losses result in lower thermal efficiency than other MD configurations. Also, the membrane materials used in the MD system affects the thermal efficiency of the system. Polymers with low thermal conductivity are preferred to minimize heat loss. Notably, increasing the thermal conductivity from 0.05 to 0.5 W/mK would result in a 55% reduction in thermal efficiency⁶⁰. The difference in SEC when using different types of membranes for MD systems is detailed in the study by Nassrullah et al.².

The highest SWP in Fig. 3b was from Koschikowski et al.'s study⁶¹, they developed a compacted MD system and a "two-loop" larger capacity MD system with a heat exchanger separating the seawater loop and collector loop with the SEC 100–200 kWh/m^3 , and GOR about 3–6. The use of a heat exchanger and control unit improves the system's efficiency. The lowest SWP was discovered in Ma et al.'s study⁶² where they compared and analyzed the direct solar-heating schemes for vacuum MD (VMD) by a photothermal membrane (VMD-PM) and by a solar absorber-plate (VMD-FPC) at ultra-low temperature. Unlike VMD-FPC, VMD-PM does not use the absorber-plate, instead by absorbing solar radiation and causing evaporation from the seawater input, the membrane itself can increase the solar-VMD process. As the concentration ratio (CR) changes from 1 to 4, the SECs of VMD-PM and VMD-FPC decrease, and the thermal efficiency rises from 76.5% to 78.1% (VMD-PM) and 73.2% to 76.8% (VMD-FPC). The cause was associated with the observation that the operating temperatures did not rise linearly with increased solar energy inputs. Consequently, although heat loss escalated at higher CRs, its share of the total received solar energy reduced, resulting in improved thermal efficiency. However, they elaborated that improvements resulting from the use of solar-absorbing PM compared to MD modules heated with solar absorber-plates have still not been quantitatively recognized, and one of the biggest challenges to improving the efficiency of the energy-intensive MD process is still the low intensity of solar radiation.

From Fig. 4a, it can be extrapolated that the overall SEC of MD is extremely higher than other technologies and the energy efficiency is limited by the thermal separation of salt from water⁶³. The diverse data on MD

systems makes it difficult to conclude their energy consumption, especially considering the varied SEC due to different MD types. Consequently, no clear trend of increasing efficiency over time is evident (Fig. 3b). Among different MD configurations, AGMD tends to have better energy efficiency because of the improved heat recoveries compared to other MD systems^{64,65}. DCMD systems exhibit enhanced energy efficiency when integrated with heat exchangers capable of transferring heat from permeate or retentate to feed water, or when employing high-performance membranes or multi-stage configurations^{66,67}. Despite MD requiring much higher energy consumption than RO, its capacity for desalinating very high salinity water up to 200,000 ppm makes it advantageous. Future development of MD should focus more on system and membrane design to increase energy efficiency, either to recover the latent heat to lower the heat demand from the energy consumption side or to multiply the total amount of heat input from the energy source side by solar concentration.

Using waste heat (WH) as the energy source is promising for driving the MD process to heat the feed water to achieve the desired temperature. MD requires low-grade WH, which is both abundant and feasible to utilize^{68,69}. Additionally, the use of WH in desalination can reduce energy consumption, GHG emissions and overall cost to 22–23%². Using WH for brine concentration in thermal desalination can mitigate and control brine disposal, and maximize the desalination recovery⁷⁰.

Direct solar desalination

Direct solar desalination uses passive or active solar stills to convert solar energy into distilled water directly⁷¹. Many advanced materials and novel ways have been developed to enhance solar-to-vapor conversion efficiency in direct desalination, leading to a sharp improvement in SWP (Fig. 4b).

Kabeel used a solar still with a jute concave wick surface that can increase the solar radiation absorption and evaporation surface area, which has a maximum SWP of 0.5 L/m²h and an efficiency of 30%⁷². Zhu et al. constructed a black titania nanocages film that enhances the total absorption because of the light trapping effect and can reach a solar-to-heat conversion of 70.9% with 1.13 L m⁻² h⁻¹ water production rate under one sun illumination⁷³. Finnerty et al. used a synthetic leaf that is composed of graphene oxide thin film material for water vapor generation with zero liquid discharge⁷⁴. They demonstrated outstanding stability in high salinity water as well as broadband light absorption, and the water production rate is 2 L m⁻² h⁻¹ with an efficiency of 78% under 0.82-sun illumination. Wang et al. constructed a 3-stage Spectrally Selective Absorber material -MD that can recycle the latent heat of water vapor with a SWP of 2.78 L m⁻² h⁻¹ and solar-to-vapor efficiency of 195%⁷. Xu et al. recently developed a ten-stage, low-cost and salt-accumulation-free thermally-localized multistage solar still that has a record-high solar-to-vapor efficiency of 385% with a SWP of 5.78 L m⁻² h⁻¹ under 1-sun illumination⁷⁵.

Several reasons could explain why direct solar desalination shows clear progress in efficiency. To improve the SWP of direct solar desalination, most of the studies focused on improving the efficiency of solar energy utilization. It can be realized by enhancing the solar absorbers' absorptivity, such as material innovation and interfacial solar heat localization and the thermal efficiency of vapor generation⁷². However, the solar-to-vapor conversion efficiency is capped below 100%. To break through 100%, harvest and reuse the vaporization enthalpy needs to be considered, which is already achieved in previous studies. Also, direct solar desalination seems to be less affected by the feed water salinity and plant scale variation as they are mostly small-scale devices. However, STD systems with large scale tend to have high efficiency but it can be hardly shown when applied to small scale. Some innovations on large-scale STD may not be practical or economically viable for small-scale applications⁴. This also explains the fluctuating indirect solar desalination data in Fig. 4, as our data cover a wide range of plant capacities. In addition, certain solar desalination systems face challenges due to mismatch between high-temperature solar collector technology and single desalination modes, resulting in decreased efficiency—a concern less prevalent in direct solar desalination systems⁴. Another reason is the standardized metrics, including the solar-to-vapor conversion efficiency equation Eq. 2 and water

production rate, making it easy to track and compare between different studies.

$$\eta = \frac{\dot{m}h_{fg}}{q_{solar}A} \quad (2)$$

Where \dot{m} is the vapor production rate under steady state, h_{fg} is the water evaporation enthalpy, q_{solar} is the input solar flux, and A is the effective solar absorbing area.

It seems very promising for direct solar desalination to further enhance efficiency and productivity. Despite the current direct solar desalination is small-scale, it has the potential to apply in a large-scale application in the future.

A transferable learning from solar systems to solar desalination

Based on the analysis of cost and efficiency data for solar desalination from both literature and commercial plant databases, improvements have been observed, though they are not as pronounced as those in other clean energy sectors such as solar, wind, or batteries. In this section, we examine the learning rates of solar energy and lithium-ion battery development in the past several decades, and apply these insights to the development of solar desalination. This approach helps us understand what actions can accelerate the advancement of solar desalination.

Learning curve

Learning curve of PV and lithium-ion batteries. The learning curve is a valuable tool for predicting technical changes and providing information for energy technology policy decisions. The model describes the relationship between the cumulative production of technology and its cost, and the learning rate is the rate at which certain costs decrease for each doubling of cumulative experience^{17,18,76}. The concept was first adopted in aircraft industries and later has been applied in a variety of areas, such as solar photovoltaic modules and lithium-ion batteries.

The solar PV and lithium-ion battery sectors have experienced significant cost reductions, which have been tracked and substantiated through the learning curve approach. This method not only tracked these achievements but also provided insights into their success and spurred further cost decreases. The PV industry, for example, has demonstrated a learning rate of approximately 24%, with the cost of solar PV modules declining by 80% since 2008, according to Liebreich et al.⁷⁷. Similarly, lithium-ion battery storage used in electric vehicles has shown a learning rate of 16%, as reported by Luo et al.⁷⁸. The learning curves for both PV and battery technologies are illustrated in Fig. 6.

Kittner et al. showed a conventional one-factor lithium-ion battery storage learning rate of 17.31% for economies of scale and 15.47% for experience curve^{79,80}. However, the traditional one-factor learning curve can solely explain the PV cost reduction caused by increases in the installed capacity or cumulative production, while it overlooks the other factors such as R&D investment, customer feedback (learning-by-using) and spill-over effects (learning-by-interacting).

Hong et al. considered a two-factor model: cumulative power generation and R&D investment, which reflects the effects of supplier-oriented R&D investments in key government policies⁸¹. The results show that the cost was reduced by 2.33% for every doubled cumulative PV power generation and 5.13% for every doubled R&D investment. Similarly, Kittner et al. applied a two-factor learning curve, which has a learning rate of 16.9% for economies of scale and a price reduction rate of 2% per Patent Cooperation Treaty patents⁷⁹. The comparison between traditional and two-factor learning curves is shown in Fig. 6b, and it demonstrates the traditional model overestimated the prices from 2010–2015. From the two-factor model, one of the drivers for cost reduction is innovation which is a key component for technology learning, and they believe that innovation contributes more to cost reduction than deployment. A multifactor learning curve model was also developed for Li-ion NMC battery packs. Among the

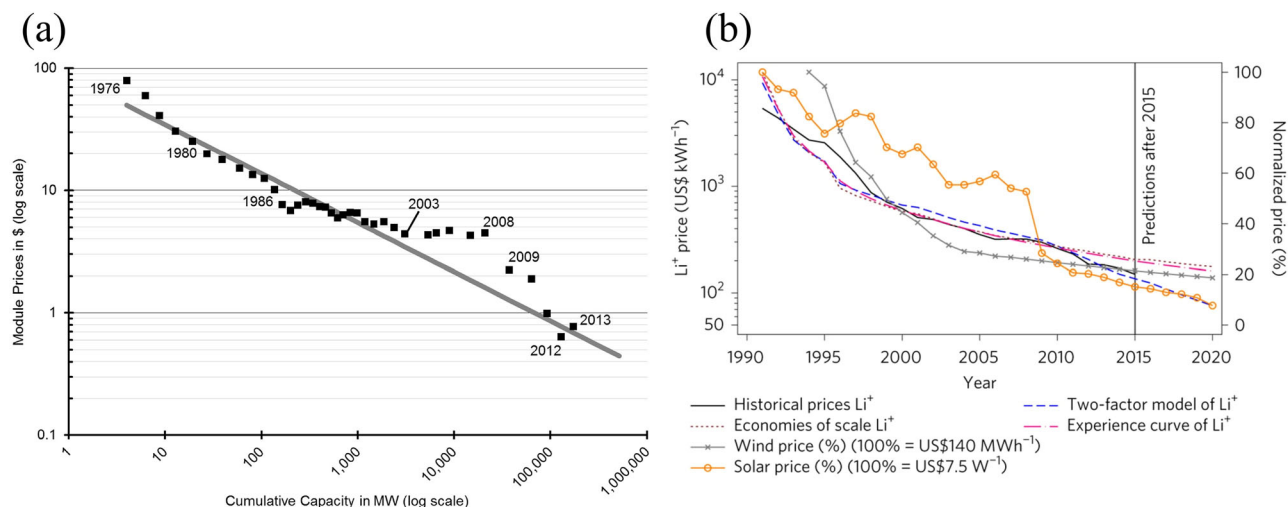


Fig. 6 | Solar PV module learning curve and model comparison for historical price prediction. **a** Solar PV module learning curve (Reprinted with permission from ref. 114). **b** Comparison between traditional one-factor learning curve models with the two-factor models to historical prices (Reprinted with permission from ref. 79).

generated models, the two-factor learning curve was proved to be realistic, with a learning rate of 21.81% for battery demand and 3% for innovation⁸². They also used the learning curve results for predicting the optimum LCOE.

Nemet stated that the traditional learning curve only weakly explains changes in the three most significant factors of cost reduction: module efficiency, plant size and silicon cost¹⁷. To explain the cost reduction reasons beyond the learning curve, the study developed a cost model that consists of silicon cost, module efficiency, plant size, yield, poly-crystalline share, silicon cost and consumption, and wafer size to simulate effects of factors' changes on manufacturing cost in each year. From 1980–2001, the plant size, efficiency and silicon cost accounted for 43%, 30% and 12% of the PV cost reduction. This result aligns with Kavlak et al.'s study⁸³ that module efficiency improvement contributed the most to the cost reduction in 1980–2001, while the difference from Nemet's study¹⁷ was that cost-reducing effects not only concentrated on plant size and module efficiency, but also other variables. Kavlak et al. developed a cost model that includes different variables (low-level mechanisms of cost reduction) and attributed them to high-level mechanisms (R&D, learning-by-doing, and scale economies)⁸³. Private and government-funded R&D was the most important high-level mechanism from 1980–2012, while after 2001, economic scales was a significant reason for cost reduction. The R&D and economies of scale accounted for 59% and 22% of the cost reduction, respectively, however, learning-by-doing only contributed 7%. Policies to stimulate market growth through privately funded R&D and economies of scale, and to a lesser extent learning-by-doing, have played a key role in lowering PV costs. The basic model Eqs. 3–6 and two-factor model Eq. 7 are shown in below.

$$Cost_t = Cost_{t_0} \times Q^\alpha \quad (3)$$

$$PR = 2^\alpha \quad (4)$$

$$LR = 1 - 2^\alpha \quad (5)$$

$$\log Cost_t = \log Cost_{t_0} + \alpha \times \log Q \quad (6)$$

$$\log Cost_t = \log Cost_{t_0} + \alpha \times \log Q + b \times \log K \quad (7)$$

where $Cost_t$ is the unit cost at time t , $Cost_{t_0}$ is the initial unit cost, Q is the cumulative production or installed capacity, PR is the progress ratio, α is the learning coefficient. Since Eq. 3 is an exponential form, Eq. 3 can be converted to Eq. 6. K is the second factor considered in two-factor model and b is the corresponding learning coefficient.

Learning curve of desalination. To date, only three studies have investigated the learning curve concept in the desalination field. Caldera and Breyer developed the first learning curve for SWRO plants to analyze the historical patterns of SWRO capital expenditures (CAPEX) as the historic global cumulative online SWRO capacity increases⁸⁴. They used the log-linear model that focused on “learning by doing” and predicted the SWRO CAPEX till 2050 based on the learning rate. The model can be found from Caldera and Breyer⁸⁴.

The learning rate of SWRO plants was 15% from 1977 to 2015, which implies for every doubling of cumulative online SWRO capacity, SWRO CAPEX decreased by 15% (Fig. 7a). Before 2004, the global average CAPEX reduction corresponded with 15% of the learning rate. However, the average CAPEX value declines from the learning curve after 2004 because of the economy of scale effect. This is due to the increase in the number of large and extra-large SWRO capacities as a result of the development and commercialization of large-diameter RO membranes⁸⁵. Nevertheless, due to the location-specific parameters and the globally spread SWRO plants that affect the CAPEX, the sudden rise in CAPEX can also be observed in some years.

However, the lack of consideration of scale effect in Caldera and Breyer's study may lead to the overestimation of the learning effect⁸⁴. Mayor separated and analyzed the “economies of scale” and “learning by doing” effects on historical cost reductions for MED, MSF and RO⁸⁶. The economies of scale effect was estimated by using Eq. 8 below. Economies of scale have the greatest impact on MED with a scale coefficient of 0.71.

$$Cost_2 = Cost_1 \times \left(\frac{Size_2}{Size_1} \right)^p \quad (8)$$

where cost is the absolute investment cost and size is the total sizes of plant 1 and 2. p denotes the exponential scale coefficient. $p < 1$ means the positive economies of scale effects, which is larger scales lead to specific cost reduction.

Additionally, they used a “de-scaled” learning curve model from Eq. 9 to derive the learning rates for the three desalination technologies⁸⁷. The “de-scaled” method gives more accurate estimations as the effect of unit scaling was detached when estimating the learning. Also, because the unit scale and learning experience were separated, the cumulative capacity measured in the same unit became clearer. When excluding the effects of scale, the de-scaled learning rate is 23%, 30%, and 12% for MED, MSF, and RO, respectively. The results show that learning has been the dominant reason driving

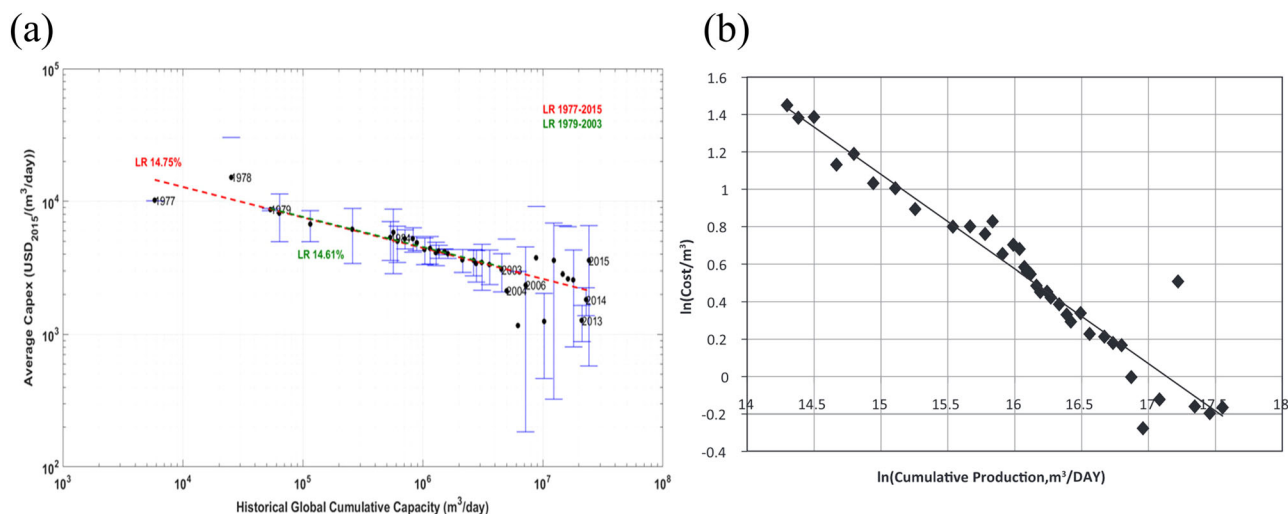


Fig. 7 | Learning curves of SWRO and desalination plants. a SWRO learning curve from 1977–2015 and 1979–2003 (Reprinted with permission from ref. 84). **b** Desalination Learning Curve for Global Data (Reprinted with permission from ref. 89).

historical desalination cost reductions.

$$Cost_t = Cost_{t_0} \times (U_t/U_{t_0})^\alpha$$

$$LR = 1 - 2^\alpha \quad (9)$$

where $Cost_t$ and $Cost_{t_0}$ are the unit cost at time t and the previous time step. U_{t_0} and U_t is the cumulative number of units at initial and the cumulative number of units installed by time t .

MSF has the highest learning rate and the intense growth stage occurred in 1970 when a surge of MSF in Middle Eastern industrial deployment quickly surpassed MED. The rapid cost reduction phase was due to the competition among different desalination technologies, technical enhancement and knowledge sharing throughout projects as well as an increase in the flexibility of build-own-operate-transfer contracts resulting in more design and optimization flexibility as bidders can create costing strategies that minimize total plant life costs (including operation) rather than plant building costs⁸⁸. The intense learning phase of RO was from 1975 to 2006, which aligns with the reasons mentioned in the previous section, that is the efficiency improvements in energy use and membrane performance.

The traditional learning rate of RO (15%) in Caldera and Breyer's study⁸⁴ is slightly different from Mayor's study⁸⁶, however, the learning rate in Sood and Smakhtin's study is proved to be overestimated. Sood and Smakhtin were the first who develop a desalination learning curve, by integrating MED, MSF and RO. So far, only they consider the PV desalination learning curve by combining the existing PV learning curve with the desalination learning curve⁸⁹. The cost of energy for desalination was taken out from the total cost of desalination as a measure of output when developing the learning curve and the desalination learning curve is shown in Fig. 7b, with the learning rate of 29%. However, the learning curve result is overestimated especially for MED and RO, as they joint measured the three technologies without differentiating the strong differences among the technology types and the CAPEX and operational costs (OPEX) effect as well as not considering the economies scale⁸⁴. Also, as they used the integrated desalination learning rate when combined with the PV learning rate, the result could be inaccurate. The PV should be combined with RO only and the involvement of thermal desalination might lead to an overestimation.

Transfer the learning from PV and battery to solar desalination. Since PV and batteries experienced a significant cost reduction over the years, it is possible to transfer their cost reduction factors from the learning curve

into solar desalination pointing out the pathway for cost reduction in the future. Also, lithium-ion batteries, as a key energy storage medium in the solar desalination systems for solar power when there are excess PV energy production, highlight promising trends for enhancing the viability of solar energy by providing a consistent energy supply when sunlight is unavailable. There are other batteries used in the solar desalination, such as lead-acid battery storage system which has low capital cost compared to other systems⁹⁰.

Currently, solar desalination plants are primarily lab-scale ($<1 \text{ m}^3/\text{day}$) and pilot-scale ($20\text{--}1200 \text{ m}^3/\text{day}$), with sizes not yet reaching the large scale typical of commercial desalination plants such as industrial or municipal scale systems^{54,91}. This disparity suggests that economies of scale may not yet play a significant role in reducing costs for solar desalination. The reduction in silicon costs, a major factor in lowering PV costs, could similarly influence cost reduction efforts for solar desalination. Indeed, the costs of key components, including membranes, PV panels, and solar collectors, have decreased in the past. To discern whether these reductions stem from learning effects or changes in commodity prices, a two-factor model could be employed.

Additionally, while module efficiency improvements have been crucial for PV cost reductions, our findings suggest that overall system efficiency in solar desalination does not consistently improve alongside PV efficiency. Thus, this factor may not directly lead to cost savings in solar desalination. On the other hand, as SEC of RO plants on a downward trend, nearing a critical threshold, future research should **prioritize developing methods to integrate desalination systems with fluctuating solar energy sources**, thereby enhancing the overall efficiency and resilience of these systems. Continuing efficiency improvements in both solar energy generation and water desalination, and effectively merging them to optimize solar-to-water conversion, could unlock considerable potential. Recent advancements in membrane materials with plasmonic photothermal components for membrane distillation have significantly improved system performance. These materials reduce temperature polarization, enhance light-to-heat conversion efficiency, and lower energy consumption, leading to reduced OPEX⁹². This scalable process is feasible for producing sufficient water for households and communities, with potential for further cost reductions⁹³. Improved integration between solar and desalination stands to gain substantially from historical achievements in both the solar energy and desalination sectors.

Although detailed statistics on the global count of commercial solar desalination plants are not currently accessible, it's evident that their installed capacity significantly trails behind that of PV, batteries, or traditional desalination technologies. This disparity highlights the substantial potential for cost reductions through learning-by-doing at this stage.

Recognizing system integration as a crucial factor, leveraging successes from both the solar energy (including PV and solar thermal) and desalination sectors becomes paramount. Continuous studies and practical optimization of operations to enhance the utilization of fluctuating solar energy are essential. Innovations aimed at boosting overall energy efficiency and enabling the effective use of solar energy—without escalating water costs—appear as a promising yet underexploited opportunity through learning-by-doing. This would be stimulated and driven by the decreasing costs of solar energy and the demand in addressing water scarcity without generating CO₂ emissions.

Moreover, an essential lesson from the PV and battery sectors is the importance of tracking and analyzing the learning curves of solar desalination across different application scenarios and technological paths. The cost of water production can vary significantly across various system scales, water salinities, locations and desired qualities of the produced water. These variables introduce complexity and challenges in developing a comprehensive learning curve for solar desalination, including issues related to data collection and inconsistencies in academic research. It is recommended to create distinct learning curves for PV-RO systems handling seawater and brackish water. Upon establishing these learning curves, the model could be enhanced by employing a two-factor analysis to explore additional factors driving cost reductions, such as R&D (learning through innovation/research), knowledge spillovers, and market dynamics. Elevating R&D investments is crucial for achieving technological competitiveness, especially in the initial stages of development. While these investments are significantly effective early on, their impact tends to decrease as the technology progresses towards demonstration and commercialization stages⁹⁴. Crucially, a deep understanding of the learning curve for solar desalination will illuminate the sector's global potential over the coming decades. Linking the learning curve of solar desalination's CAPEX with the lifetime water cost offers a predictive view of future water costs, underpinning strategic decisions in the sector.

Additionally, it is important to consider brine management in the overall desalination process, as the unsustainable and high capital cost of brine disposal remains a significant challenge. Although previous studies on the learning curve of solar desalination have often overlooked brine disposal costs, this expense is a key factor that can hinder the economic feasibility of desalination⁹⁵. Therefore, future studies must incorporate brine disposal costs to provide a comprehensive assessment. Furthermore, conducting a life cycle assessment (LCA) alongside a techno-economic assessment is crucial for evaluating the overall sustainability of solar desalination systems, encompassing energy consumption, greenhouse gas (GHG) emissions, and broader environmental impacts, given the energy-intensive nature of desalination processes and the potential for solar energy to mitigate climate change.

Standardize metrics for the tracking of cost and efficiency

Solar desalination water cost. The concept of Levelized Cost of Electricity (LCOE) has been introduced in the calculation of desalination water cost. LCOE shows the total costs of electricity over the project's economic life or entire life and is commonly used to assess the feasibility and competitiveness among different electricity generation technologies⁹⁶. The general calculation is shown below:

$$LCOE = \frac{\text{Lifecycle cost}}{\text{Lifetime electricity production}} \left(\frac{\$}{\text{kWh}} \right) \quad (10)$$

Similarly, **levelized cost of water (LCOW)** is an economic metric used for comparing the system lifetime cost among various solar desalination technologies with different plant sizes, configurations, etc¹⁹.

$$LCOW = \frac{I_0 + \sum_{t=1}^n \frac{C_t}{(1+i)^t}}{\sum_{t=1}^n \frac{M_{w,t}}{(1+i)^t}} \quad (11)$$

where C_t denotes the annual cost of operation and $M_{w,t}$ is the water production in year t .

To simplify LCOW, most papers adopt Simplified Cost of Water (SCOW) (Eqs. 12 & 13) by using an “amortization factor”. In SCOW, it is assumed that the water production and the running costs for each year are the same, which is fair as they assume the system performance is stable. The detailed versions of SCOW and LCOW give practically the same results in most cases when sufficient simplicity is taken into account⁹⁷.

$$SCOW = \frac{CRF \times CAPEX + OPEX}{V_{\text{water}}^{\text{year}}} \quad (12)$$

$$CRF = \frac{i(1+i)^n}{(1+i)^n - 1} \quad (13)$$

Also, it is common to break down the OPEX cost into fixed OPEX and variable OPEX which is the LCOE as shown in Eq. 14 that is used in the learning curve⁸⁴. Furthermore, the simplest calculation of cost of water (COW) Eq. 15 was also used in some studies where no consideration of future cash flow discounting^{98,99}.

$$SCOW = \frac{CAPEX \times CRF + OPEX_{\text{fixed}}}{\text{Total water production in a year}} + (LCOE \times SEC) \quad (14)$$

$$COW = \frac{\left(\frac{CAPEX}{n} \right) + OPEX}{V_{\text{water}}^{\text{year}}} \quad (15)$$

where CRF is the capital recovery factor to convert the initial CAPEX to annual CAPEX and it applies a discount rate (i) over a compounding period (n) to compute the present value of an annuity¹⁰⁰. CAPEX is the capital expenditure of the solar desalination system and OPEX is the operating expenditure. $V_{\text{water}}^{\text{year}}$ is the annual total volume of water production (assume same for every year). $OPEX_{\text{fixed}}$ is the fixed OPEX of the desalination plant, LCOE is the levelized cost of electricity in \$/kWh and SEC is the specific energy consumption in kWh/m³.

The variation of cost models used and cost components considered in different studies, which is also one of the reasons for cost variation in Section “Efficiency trend of solar desalination in prior studies”. Even for software packages and tools such as SWRO cost estimator and DEEP, their accuracy varies with error ranges of ± 10 to 50% for different RO and thermal desalination plants^{101,102}.

Siting also significantly affects the cost modelling. This causes the cost data reported to be commonly not consistent for different technologies or similar-sized facilities. The electricity prices can vary significantly worldwide. For instance, the Emirate has developed the cheapest-on-earth solar PV power plant, which has an electricity price of 2.48\$/kWh and is significantly lower than the price in many places in the world¹¹. To improve the accuracy of LCOE due to the location-specific, location-based cost adjustment factors that take into account varying living costs and remote location-related expenses were used to calculate capital costs in different regions. By using the cost adjustment, the cost in remote locations including productivity and labor differences are solved¹⁰³. A map-based LCOE calculator with regional multipliers was developed for region-specific CAPEX and O&M data¹⁰⁴.

To improve the effectiveness of the cost modelling, the cost mentioned above models were purposefully selected for varied focused calculations or comparisons. Papapetrou et al. gave a guidance on how to formulate these cost models for purposes such as 1). Desalination configuration comparison. 2). Desalination technologies comparison. 3). Water supply options comparison. 4). Investment options comparison (details are in Supplementary Table 1)⁹⁷.

So far, we found that SCOW dominates the solar desalination literature (either comparing configurations or desalination technologies), while few paper use LCOW and NPV. However, if future studies will focus on comparing water supply options and investment options, the LCOW method

can be adopted from desalination studies. For the future development of solar desalination technologies and fair cost comparison, it is necessary to determine the components and complexity of cost models and purposes. Methodologies for estimating water costs must identify and specify every factor that affects the cost of desalination and create a transparent, organized process for estimating the cost of desalinated water for any given facility¹⁰⁵. A standardized cost calculation should be developed for the MD system to compare with other well-developed desalination technologies for their economic viability. Also, due to the site-specific, accuracy improvement method can be learned from LCOE and regional cost factors may be determined based on statistical methods to correct cost variances. As SCOW Eq. 14 can be separated into CAPEX and electricity cost, it is possible to reduce regional influence by adjusting the LCOE. An international/transnational reporting standard for SCOW of solar desalination is necessary to be set up.

In terms of the cost model used in learning curves, previous studies on desalination used the system's CAPEX which is the same as the PV using unit capital cost. However, Neij et al. suggested that the cost of electricity offers a more holistic gauge of technological advancement compared to the capital cost¹⁰⁶. This is because the competitive edge of technology fundamentally hinges on choices made regarding electricity expenses. If applying this idea to solar desalination, SCOW as the cost model in the learning curve seems to be more reasonable. The controversial part is Caldera and Breyer only used the CAPEX in the SCOW model and separated the electricity cost to mitigate the regional variation⁸⁴. Future studies using SCOW should account for regional factors to ensure a more accurate assessment.

Unified metric for solar desalination efficiency. The most common metrics for measuring energy consumption of solar desalination are SEC, performance ratio (PR) and GOR. However, these metrics cannot be used for a fair comparison of different desalination technologies with various grades or forms of energy. For instance, for a GOR of 9 MED and MSF plants, the thermal energy requirements of these two are not the same. Also, the metrics cannot represent the whole solar-to-water process. SWP is an important metric to measure the overall efficiency of the STD systems from solar to water conversion process. The SWP equation is shown in Eqs. 16–19. It is originally used for comparison between STD systems, however, after the derivation of Eq. 17, with the SEC value we can use Eq. 16. to compare the solar-to-water overall performance between electrically-driven solar desalination and STD systems⁷.

$$SWP = \frac{E\eta_s}{SEC} \quad (16)$$

where E is the solar irradiance (kW m^{-2}), which is assumed as 1000 W m^{-2} in this study. η_s is the solar utilization efficiency for evaporation. The solar energy utilization efficiency for PV and STD systems typically ranges from 12–25% and 60–90%, respectively^{7,107,108}. Thus, in this study, the η_s of PV and STD systems were assumed as 20% and 75%, respectively. SEC is the specific energy consumption for the generation of a unit volume of water (kWh/m^3)

$$SWP = \frac{E}{L} GOR_{STD} = \frac{E}{L} \eta_c \eta_t GOR \quad (17)$$

$$\eta_s = \eta_c \eta_t \quad (18)$$

$$SEC = \frac{L}{GOR} \quad (19)$$

where η_c is the solar collector system efficiency for converting from solar energy into thermal, η_t denotes the heat transfer efficiency for using the thermal energy to evaporate the water, GOR is the gained output ratio, L is the energy needed to evaporate 1 liter of saline water.

However, when SWP is unavailable to calculate, an alternative metric is the equivalent universal performance ratio (UPR_{equiv}). UPR can be used to compare different desalination systems including membrane-based, thermally-driven and humidification-dehumidification that are powered by the same primary energy source. This can be achieved by invoking the second law of thermodynamics, which states that the equivalent work of the separation process is achieved by providing primary energy¹⁰⁹. UPR is a derived metric from primary energy (PE) which is the fairest metric to compare the energy consumption of any combination of power plants with desalination technologies under the same energy source. It also bridges the energy consumption with the operating cost. For solar-powered desalination, it can be converted to solar radiation by dividing the appropriate efficiency¹¹⁰.

The UPR was first proposed by Wakil Shahzad et al.¹⁰⁹ and calculated based on Eq. 20.

$$UPR = \frac{\text{evaporative energy}}{\text{primary energy input}} = \frac{h_{fg,vapor}}{3.6 \left\{ CF1 \left(\frac{\text{kWh}}{\text{m}^3} \right)_{\text{electrical}} + CF2 \left(\frac{\text{kWh}}{\text{m}^3} \right)_{\text{Thermal}} + CF3 \left(\frac{\text{kWh}}{\text{m}^3} \right)_{\text{renewable}} \right\}} \quad (20)$$

where CF is the conversion factor and $h_{fg,vapor}$ is the equivalent vapor energy

$$TL = \frac{h_{fg,vapor} \left(\frac{\text{kJ}}{\text{kg}} \right)}{\text{Minimum separation energy} \left(\frac{\text{kJ}}{\text{kg}} \right)} = \frac{2326}{2.8} = 828 \quad (21)$$

where TL is the thermodynamic limit of UPR, $h_{fg,vapor}$ is the latent heat vaporization for water 2326 kJ/kg, minimum separation energy is converted from the minimum separation work 0.78 kWh/m³.

However, the calculated UPR values alone do not provide a comprehensive understanding unless compared with the thermodynamic limit for the separation. The thermodynamic limit of UPR (Eq. 21), defined as the ratio of evaporation energy to the minimum separation energy, is 828. This is based on the minimum separation work of 0.78 kWh/m³ at 35,000ppm concentration¹⁰⁹. When the UPR values for RO, MSF, and MED are 86, 60, and 88, respectively, the corresponding percentages of the thermodynamic limit are 10.4% for RO, 7.2% for MSF, and 10.6% for MED. These findings highlight that all desalination processes operate at only 10–13% of the thermodynamic limit of UPR, which is extremely unsustainable for water resources in the future¹⁰⁹. The UPR trend for over 40 commercial desalination plants (SWRO, MSF and MED) in Shahzad et al.'s study indicates a gradual improvement in the efficiency over the past 3 decades (Fig. 8)¹⁰⁹. An improvement of UPR from 113 to 175 in Fig. 8 can be observed due to the

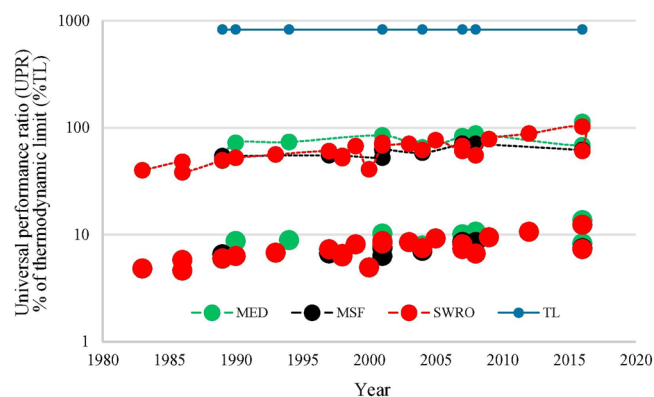


Fig. 8 | UPR changes and thermodynamic limit of UPR of 40 World desalination plants over last 3 decades (TL: thermodynamic limit). UPR value is calculated from Eq. 20. The dot points linked with the dashed line are the UPR values of MED, MSF and SWRO. The dot points (% of TL) are the ratio of UPR for MED, MSF and SWRO to the thermodynamic limit of UPR (Reprinted with permission from ref. 109).

hybridization of MED with the adsorption process. Same as SEC, the UPR is also affected by the salinity of feed water. However, the difference is the maximum UPR can be achieved when the salinity is lower. Subsequently, Zheng et al. proposed an adapted version of UPR, which is UPR_{equiv} in Eqs. 22–23. UPR_{equiv} takes into account the specific equivalent electricity consumption (SEC_{equiv}) and reference latent heat of evaporation²⁶.

$$UPR_{equiv} = \frac{h_{ref}}{CF_{KJ,kWh} SEC_{equiv}} \quad (22)$$

$$SEC_{equiv} = SEEC + STEC \times \eta_{cdt} \quad (23)$$

where $CF_{KJ,kWh} = 3.6$, is a conversion factor for kJ/kg to kWh/m³, h_{ref} denotes a constant reference value representing the specific enthalpy of evaporation at 73 °C (2,326 kJ/kg), SEC_{equiv} is the specific equivalent electricity consumption of the desalination system, $SEEC$ is the specific electricity consumption and $STEC$ is the specific thermal energy consumption, η_{cdt} is the average electricity efficiency for electricity generation, distribution and transmission, which is used for acquisition of electrical energy equivalent to thermal energy.

Nevertheless, this metric lacks precision when comparing systems powered by different primary energy sources¹¹ and it cannot be used solely but can be a complement comparison tool. However, since the comparison is only within the solar-powered desalination systems, this shortcoming could be neglected. It is important to learn from the PV cell efficiency metric and find a unified one in tracking and compare the efficiency improvements for solar desalination technologies, as it directly leads to cost savings and has the potential to spur additional advancements in technology and engineering, crucial for achieving substantial long-term cost reductions. The main challenges of solar desalination associated with their unified cost and efficiency metrics are shown in Fig. 9. In addition, when selecting desalination plants, the factors to determine are usually not SEC, exergy consumption, GOR, or primary energy consumption, instead the key determining factor is LCOW as bids will be won by the company that can produce water at the lowest cost while adhering to all performance, environmental, legal, and geographical requirements¹¹.

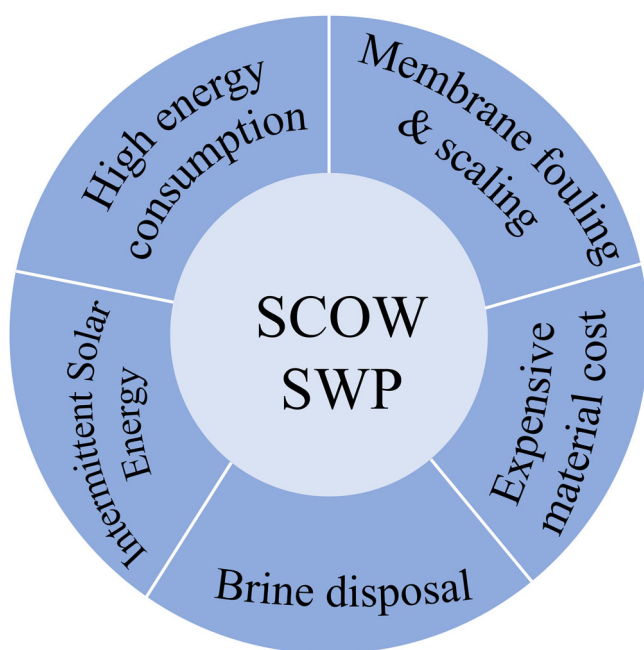


Fig. 9 | Solar desalination challenges and unified metrics for water cost and efficiency. The scheme summarizes the key challenges and unified metrics (SCOW and SWP) for water cost and efficiency in solar desalination.

Conclusion

Solar desalination has rapidly developed over the past decades; however, it faces limitations such as high costs and low efficiency. The current challenges of solar desalination and the unified metrics are summarized in Fig. 9. This paper provides a comprehensive review and analysis of research prioritizing cost and efficiency, focusing on electrically-driven, thermally-driven, and direct solar desalination technologies. Over the last four decades, the water cost of solar desalination has decreased, yet there was no significant upward trend in the solar-to-water efficiency except for many solar desalination technologies. The cost reduction is primarily attributed to technical improvements in PV panels, solar collectors, and membrane designs, along with integrated processes and market competition. We identify that the efficiency of desalination systems is significantly influenced by feed water salinity, plant size, system designs, and membrane properties. As our found SEC data is collected from previous studies, each with different situations and assumptions, the inconsistency makes it challenging to identify a chronological trend in efficiency improvement over the last 40 years, but this does not necessarily imply a lack of progress. To verify the progress across solar desalination studies and accelerate the technology's development and deployment, lessons could be learned from the rapidly developed PV and Li-ion battery industries through the learning curve concept. However, we identify a gap in the learning curve for solar desalination and suggest initially developing learning curves for different use scenarios, then creating two or multi-factor models to analyze other cost-reduction factors. Accurate, unified metrics for cost and efficiency are crucial for solar desalination's development. Among the many metrics used, we highlight that SCOW and SWP are two metrics that allow for fair comparisons across different solar desalination technologies. SCOW could serve as the cost model for the solar desalination learning curve but must account for regional effects. This paper aims to guide researchers and engineers in future solar desalination development towards cost reduction and efficiency improvement. LCA is beyond our study's scope, future studies should carry on LCA of various solar desalination technologies with the consideration of brine disposal to assess the overall sustainability of the solar desalination processes.

Data availability

All data supporting the findings of this study are available within the paper and its Supplementary Information and Supplementary Data 1 & 2. The DWI DesalData is available at <https://www.desaldata.com/>. The original best Research-cell efficiency data that supports the Fig. 5 is available at <https://www.nrel.gov/pv/cell-efficiency.html>.

Received: 29 February 2024; Accepted: 19 September 2024;
Published online: 30 September 2024

References

- He, C. et al. Future global urban water scarcity and potential solutions. *Nat. Commun.* **12**, 4667 (2021).
- Nassrullah, H., Anis, S. F., Hashaikeh, R. & Hilal, N. Energy for desalination: A state-of-the-art review. *Desalination* **491**, 114569 (2020).
- Ali, M. T., Fath, H. E. S. & Armstrong, P. R. A comprehensive technological review of indirect solar desalination. *Renew. Sustain. Energy Rev.* **15**, 4187–4199 (2011).
- Huang, J., Zheng, H. & Kong, H. Key pathways for efficient solar thermal desalination. *Energy Convers. Manag.* **299**, 117806 (2024).
- Ahmed, F. E., Hashaikeh, R. & Hilal, N. Solar powered desalination – Technology, energy and future outlook. *Desalination* **453**, 54–76 (2019).
- Esmailion, F. Hybrid renewable energy systems for desalination. *Appl Water Sci.* **10**, 84 (2020).
- Wang, Z. et al. Pathways and challenges for efficient solar-thermal desalination. <https://doi.org/10.1126/sciadv.aax0763> (2019).

8. Laborde, H. M., França, K. B., Neff, H. & Lima, A. M. N. Optimization strategy for a small-scale reverse osmosis water desalination system based on solar energy. *Desalination* **133**, 1–12 (2001).
9. Karanikola, V. et al. Economic performance of membrane distillation configurations in optimal solar thermal desalination systems. *Desalination* **472**, 114164 (2019).
10. Ranjan, K. R. & Kaushik, S. C. Economic feasibility evaluation of solar distillation systems based on the equivalent cost of environmental degradation and high-grade energy savings. *Int. J. Low.-Carbon Technol.* **11**, 8–15 (2016).
11. Kaya, A., Tok, M. E. & Koc, M. A Levelized Cost Analysis for Solar-Energy-Powered Sea Water Desalination in The Emirate of Abu Dhabi. *Sustainability* **11**, 1691 (2019).
12. Panagopoulos, A., Haralambous, K.-J. & Loizidou, M. Desalination brine disposal methods and treatment technologies - A review. *Sci. Total Environ.* **693**, 133545 (2019).
13. Alhaj, M. & Al-Ghamdi, S. G. Why is powering thermal desalination with concentrated solar power expensive? assessing economic feasibility and market commercialization barriers. *Sol. Energy* **189**, 480–490 (2019).
14. Effendi, Y. Three years experiences for PVRO-desalination. in *Conference Record of the Twentieth IEEE Photovoltaic Specialists Conference* 1194–1199 2 <https://doi.org/10.1109/PVSC.1988.105893> (1988).
15. Keeper, B. G., Hembree, R. D. & Schrack, F. C. Optimized matching of solar photovoltaic power with reverse osmosis desalination. *Desalination* **54**, 89–103 (1985).
16. Shokri, A. Techno-economic assessment of water desalination: Future outlooks and challenges. *Proc. Saf. Environ. Protect.* **169**, 564–578 (2023).
17. Nemet, G. F. Beyond the learning curve: factors influencing cost reductions in photovoltaics. *Energy Policy* **34**, 3218–3232 (2006).
18. McDonald, A. & Schrattenholzer, L. Learning rates for energy technologies. *Energy Policy* **29**, 255–261 (2001).
19. Patel, S. K., Lee, B., Westerhoff, P. & Elimelech, M. The potential of electrodialysis as a cost-effective alternative to reverse osmosis for brackish water desalination. *Water Res.* **250**, 121009 (2024).
20. Khayet, M. Solar desalination by membrane distillation: Dispersion in energy consumption analysis and water production costs (a review). *Desalination* **308**, 89–101 (2013).
21. Moore, S. E. et al. Process modeling for economic optimization of a solar driven sweeping gas membrane distillation desalination system. *Desalination* **437**, 108–120 (2018).
22. Alkhudhiri, A., Darwish, N. & Hilal, N. Membrane distillation: A comprehensive review. *Desalination* **287**, 2–18 (2012).
23. Ajiwiguna, T. A., Lee, G.-R., Lim, B.-J., Choi, S.-M. & Park, C.-D. Design strategy and economic analysis on various configurations of stand-alone PV-RO systems. *Desalination* **526**, 115547 (2022).
24. Ajiwiguna, T. A., Lee, G.-R., Lim, B.-J., Cho, S.-H. & Park, C.-D. Optimization of battery-less PV-RO system with seasonal water storage tank. *Desalination* **503**, 114934 (2021).
25. He, W., Amrose, S., Wright, N. C., Buonassisi, T. & Peters, I. M. Field demonstration of a cost-optimized solar powered electrodialysis reversal desalination system in rural India. *Desalination* **476**, 114217 (2020).
26. Zheng, Y., Caceres Gonzalez, R. A., Hatzell, K. B. & Hatzell, M. C. Large-scale solar-thermal desalination. *Joule* **5**, 1971–1986 (2021).
27. Joyce, A., Loureiro, D., Rodrigues, C. & Castro, S. Small reverse osmosis units using PV systems for water purification in rural places. *Desalination* **137**, 39–44 (2001).
28. Elimelech, M. & Phillip, W. A. The Future of Seawater Desalination: Energy, Technology, and the Environment. <https://doi.org/10.1126/science.1200488>.
29. Spiegler, K. S. & El-Sayed, Y. M. The energetics of desalination processes. *Desalination* **134**, 109–128 (2001).
30. Kim, J., Park, K., Yang, D. R. & Hong, S. A comprehensive review of energy consumption of seawater reverse osmosis desalination plants. *Appl. Energy* **254**, 113652 (2019).
31. Arenas Urrea, S., Díaz Reyes, F., Peñate Suárez, B. & de la Fuente Bencomo, J. A. Technical review, evaluation and efficiency of energy recovery devices installed in the Canary Islands desalination plants. *Desalination* **450**, 54–63 (2019).
32. Fritzmann, C., Löwenberg, J., Wintgens, T. & Melin, T. State-of-the-art of reverse osmosis desalination. *Desalination* **216**, 1–76 (2007).
33. Smith, C.B. & Parmenter, E.P. Energy management principles: applications, benefits, savings. 2nd edn. (Elsevier, 2016).
34. Voutchkov, N. *Desalination Engineering - Planning and Design*. (McGraw Hill Professional, New York, 2012).
35. Cohen, B., Lazarovitch, N. & Gilron, J. Upgrading groundwater for irrigation using monovalent selective electrodialysis. *Desalination* **431**, 126–139 (2018).
36. Song, L. et al. Emergence of thermodynamic restriction and its implications for full-scale reverse osmosis processes. *Desalination* **155**, 213–228 (2003).
37. Sagle, A. C. et al. PEG-coated reverse osmosis membranes: Desalination properties and fouling resistance. *J. Membr. Sci.* **340**, 92–108 (2009).
38. Ghaffour, N. et al. Renewable energy-driven innovative energy-efficient desalination technologies. *Appl. Energy* **136**, 1155–1165 (2014).
39. Cohen-Tanugi, D., McGovern, R. K., Dave, S. H., Lienhard, J. H. & Grossman, J. C. Quantifying the potential of ultra-permeable membranes for water desalination. *Energy Environ. Sci.* **7**, 1134–1141 (2014).
40. Ghermandi, A. & Messalem, R. Solar-driven desalination with reverse osmosis: the state of the art. *Desalination Water Treat.* **7**, 285–296 (2009).
41. Shalaby, S. M. Reverse osmosis desalination powered by photovoltaic and solar Rankine cycle power systems: A review. *Renew. Sustain. Energy Rev.* **73**, 789–797 (2017).
42. De Carvalho, P. C. M., Riffel, D. B., Freire, C. & Montenegro, F. F. D. The Brazilian experience with a photovoltaic powered reverse osmosis plant. *Prog. Photovolt: Res. Appl.* **12**, 373–385 (2004).
43. Kehal, S. Reverse osmosis unit of 0.85 m³/h capacity driven by photovoltaic generator in south Algeria. in *New Technologies for the Use of Renewable Energy Sources in Water Desalination* (Athens, 1991).
44. Herold, D. et al. Small scale photovoltaic desalination for rural water supply - demonstration plant in Gran Canaria. *Renew. Energy* **14**, 293–298 (1998).
45. Herold, D. & Neskakis, A. A small PV-driven reverse osmosis desalination plant on the island of Gran Canaria. *Desalination* **137**, 285–292 (2001).
46. Chen, Y. et al. From Laboratory to Production: Learning Models of Efficiency and Manufacturing Cost of Industrial Crystalline Silicon and Thin-Film Photovoltaic Technologies. *IEEE J. Photovolt.* **8**, 1531–1538 (2018).
47. Garg, M. C. Chapter 4 - Renewable Energy-Powered Membrane Technology: Cost Analysis and Energy Consumption. in *Current Trends and Future Developments on (Bio-) Membranes* (eds. Basile, A., Cassano, A. & Figoli, A.) 85–110 (Elsevier, 2019). <https://doi.org/10.1016/B978-0-12-813545-7.00004-0>.
48. Raval, H. D. & Maiti, S. A Novel Photovoltaic Powered Reverse Osmosis with Improved Productivity of Reverse Osmosis and Photovoltaic Panel. (2015).
49. Chehayeb, K. M. & Lienhard, J. H. On the electrical operation of batch electrodialysis for reduced energy consumption. *Environ. Sci.: Water Res. Technol.* **5**, 1172–1182 (2019).
50. Werber, J. R., Deshmukh, A. & Elimelech, M. Can batch or semi-batch processes save energy in reverse-osmosis desalination? *Desalination* **402**, 109–122 (2017).

51. Tsoutsos, T. et al. TEMPERATURE EFFECT ON PV PERFORMANCE EXPERIMENTAL RESULTS FROM A 2.18 KWP THIN FILM PV SYSTEM. in (2011).
52. Shravanth Vasisht, M., Srinivasan, J. & Ramasesha, S. K. Performance of solar photovoltaic installations: Effect of seasonal variations. *Sol. Energy* **131**, 39–46 (2016).
53. Zein, A., Karaki, S. & Al-Hindi, M. Analysis of variable reverse osmosis operation powered by solar energy. *Renew. Energy* **208**, 385–398 (2023).
54. Mohamed, E. S., Papadakis, G., Mathioulakis, E. & Belessiotis, V. A direct coupled photovoltaic seawater reverse osmosis desalination system toward battery based systems — a technical and economical experimental comparative study. *Desalination* **221**, 17–22 (2008).
55. Tafesh, A., Milani, D. & Abbas, A. Water Storage Instead of Energy Storage for Desalination Powered by Renewable Energy—King Island Case Study. *Energies* **9**, 839 (2016).
56. Sayyaadi, H. & Saffari, A. Thermoeconomic optimization of multi effect distillation desalination systems. *Appl. Energy* **87**, 1122–1133 (2010).
57. Sharon, H. & Reddy, K. S. A review of solar energy driven desalination technologies. *Renew. Sustain. Energy Rev.* **41**, 1080–1118 (2015).
58. Al-Karaghoul, A. & Kazmerski, L. L. Energy consumption and water production cost of conventional and renewable-energy-powered desalination processes. *Renew. Sustain. Energy Rev.* **24**, 343–356 (2013).
59. Deshmukh, A. et al. Membrane distillation at the water-energy nexus: limits, opportunities, and challenges. *Energy Environ. Sci.* **11**, 1177–1196 (2018).
60. Alobaidani, S. et al. Potential of membrane distillation in seawater desalination: Thermal efficiency, sensitivity study and cost estimation. *J. Membr. Sci.* **323**, 85–98 (2008).
61. Koschikowski, J. et al. Experimental investigations on solar driven stand-alone membrane distillation systems for remote areas. *Desalination* **248**, 125–131 (2009).
62. Ma, Q., Xu, Z., Wang, R. & Poredos, P. Distributed vacuum membrane distillation driven by direct-solar heating at ultra-low temperature. *Energy* **239**, 121891 (2022).
63. Brogioli, D., La Mantia, F. & Yip, N. Thermodynamic analysis and energy efficiency of thermal desalination processes. *Desalination* **428**, 29–39 (2018).
64. Summers, E. K. Experimental study of thermal performance in air gap membrane distillation systems, including the direct solar heating of membranes. *Desalination* **300**, 100–111 (2013).
65. Meindersma, G. W., Guijt, C. M. & de Haan, A. B. Desalination and water recycling by air gap membrane distillation. *Desalination* **187**, 291–301 (2006).
66. Lin, S., Yip, N. Y. & Elimelech, M. Direct contact membrane distillation with heat recovery: Thermodynamic insights from module scale modeling. *J. Membr. Sci.* **453**, 498–515 (2014).
67. Jantaporn, W., Ali, A. & Aimar, P. Specific energy requirement of direct contact membrane distillation. *Chem. Eng. Res. Des.* **128**, 15–26 (2017).
68. Elsaid, K. et al. Recent progress on the utilization of waste heat for desalination: A review. *Energy Convers. Manag.* **221**, 113105 (2020).
69. Olabi, A. G., Elsaid, K., Rabaia, M. K. H., Askalany, A. A. & Abdelkareem, M. A. Waste heat-driven desalination systems: Perspective. *Energy* **209**, 118373 (2020).
70. Elsaid, K., Sayed, E. T., Abdelkareem, M. A., Baroutaji, A. & Olabi, A. G. Environmental impact of desalination processes: Mitigation and control strategies. *Sci. Total Environ.* **740**, 140125 (2020).
71. Tiwari, G. N., Singh, H. N. & Tripathi, R. Present status of solar distillation. *Sol. Energy* **75**, 367–373 (2003).
72. Kabeel, A. E. Performance of solar still with a concave wick evaporation surface. *Energy* **34**, 1504–1509 (2009).
73. Zhu, G., Xu, J., Zhao, W. & Huang, F. Constructing Black Titania with Unique Nanocage Structure for Solar Desalination. *ACS Appl. Mater. Interfaces* **8**, 31716–31721 (2016).
74. Finnerty, C., Zhang, L., Sedlak, D. L., Nelson, K. L. & Mi, B. Synthetic Graphene Oxide Leaf for Solar Desalination with Zero Liquid Discharge. *Environ. Sci. Technol.* **51**, 11701–11709 (2017).
75. Xu, Z. et al. Ultrahigh-efficiency desalination via a thermally-localized multistage solar still. *Energy Environ. Sci.* **13**, 830–839 (2020).
76. Yelle, L. E. The Learning Curve: Historical Review and Comprehensive Survey. *Decis. Sci.* **10**, 302–328 (1979).
77. Liebreich, M. Bloomberg new energy finance summit in search of the miraculous. in (New York, NY, 2016).
78. Luo, X., Wang, J., Dooner, M. & Clarke, J. Overview of current development in electrical energy storage technologies and the application potential in power system operation. *Appl. Energy* **137**, 511–536 (2015).
79. Kittner, N., Lill, F. & Kammen, D. M. Energy storage deployment and innovation for the clean energy transition. *Nat. Energy* **2**, 1–6 (2017).
80. Schmidt, O., Hawkes, A., Gambhir, A. & Staffell, I. The future cost of electrical energy storage based on experience rates. *Nat. Energy* **2**, 1–8 (2017).
81. Hong, S., Chung, Y. & Woo, C. Scenario analysis for estimating the learning rate of photovoltaic power generation based on learning curve theory in South Korea. *Energy* **79**, 80–89 (2015).
82. Penis, X. N. et al. Projecting the Price of Lithium-Ion NMC Battery Packs Using a Multifactor Learning Curve Model. *Energies* **13**, 5276 (2020).
83. Kavlak, G., McNerney, J. & Trancik, J. E. Evaluating the causes of cost reduction in photovoltaic modules. *Energy Policy* **123**, 700–710 (2018).
84. Caldera, U. & Breyer, C. Learning Curve for Seawater Reverse Osmosis Desalination Plants: Capital Cost Trend of the Past, Present, and Future. *Water Resour. Res.* **53**, 10523–10538 (2017).
85. Voutchkov, N. *Desalination Project Cost Estimating and Management*. (CRC Press, Boca Raton, 2018). <https://doi.org/10.1201/9781351242738>.
86. Mayor, B. Growth patterns in mature desalination technologies and analogies with the energy field. *Desalination* **457**, 75–84 (2019).
87. Healey, S. Separating Economies of Scale and Learning Effects in Technology Cost Improvements. <https://iiasa.dev.local/> (2015).
88. Borsani, R. & Rebagliati, S. Fundamentals and costing of MSF desalination plants and comparison with other technologies. *Desalination* **182**, 29–37 (2005).
89. Sood, A. & Smakhtin, V. Can Desalination and Clean Energy Combined Help to Alleviate Global Water Scarcity? *JAWRA J. Am. Water Resour. Assoc.* **50**, 1111–1123 (2014).
90. Ghaithan, A. M., Mohammed, A. & Hadidi, L. Assessment of integrating solar energy with reverse osmosis desalination. *Sustain. Energy Technol. Assess.* **53**, 102740 (2022).
91. Taha, M. & Al-Sa'ed, R. Application potential of small-scale solar desalination for brackish water in the Jordan Valley, Palestine. *Int. J. Environ. Stud.* **75**, 214–225 (2018).
92. Alessandro, F., Macedonio, F. & Drioli, E. Plasmonic Phenomena in Membrane Distillation. *Membranes* **13**, 254 (2023).
93. Dongare, P. D. et al. Nanophotonics-enabled solar membrane distillation for off-grid water purification. *Proc. Natl Acad. Sci. USA* **114**, 6936–6941 (2017).
94. Rout, U., Blesl, M., Fahl, U., Remme, U. & Voß, A. Uncertainty in the learning rates of energy technologies: An experiment in a global multi-regional energy system model. *Energy Policy* **37**, 4927–4942 (2009).
95. Pinto, F. S. & Marques, R. C. Desalination projects economic feasibility: A standardization of cost determinants. *Renew. Sustain. Energy Rev.* **78**, 904–915 (2017).

96. Shen, W. et al. A comprehensive review of variable renewable energy levelized cost of electricity. *Renew. Sustain. Energy Rev.* **133**, 110301 (2020).
97. Papapetrou, M. et al. Assessment of methodologies and data used to calculate desalination costs. *Desalination* **419**, 8–19 (2017).
98. Hafez, A. & Manharawy, S. Economics of seawater RO desalination in the Red Sea region. *Egypt. Part 1. a Case Study Desalination* **153**, 335–347 (2002).
99. Lapuente, E. Full cost in desalination. A case study of the Segura River Basin. *Desalination* **300**, 40–45 (2012).
100. Turton, R. et al. *Analysis, Synthesis, and Design of Chemical Processes*. (Prentice Hall, Upper Saddle River, NJ, 2012).
101. Nisan, S. & Volpi, L. Evaluation of desalination costs with DEEP. *Int. J. Nucl. Desalination* **1**, 298–307 (2004).
102. Methnani, M. DEEP: a tool for evaluation co-generated power and desalination strategies. *Desalination* **166**, 11–15 (2004).
103. EIA. *Capital Cost Estimates for Utility Scale Electricity Generating Plants*. https://www.eia.gov/analysis/studies/powerplants/capitalcost/pdf/capcost_assumption.pdf. (2016).
104. Rhodes, J. D. et al. A geographically resolved method to estimate levelized power plant costs with environmental externalities. *Energy Policy* **102**, 491–499 (2017).
105. Ghaffour, N., Missimer, T. M. & Amy, G. L. Technical review and evaluation of the economics of water desalination: Current and future challenges for better water supply sustainability. *Desalination* **309**, 197–207 (2013).
106. Neij, L., Andersen, P. D. & Durstewitz, M. Experience curves for wind power. *Int. J. Energy Technol. Policy* **2**, 15–32 (2004).
107. Wang, Y. et al. Improved light-harvesting and thermal management for efficient solar-driven water evaporation using 3D photothermal cones. *J. Mater. Chem. A* **6**, 9874–9881 (2018).
108. Yin, X. et al. Macroporous Double-Network Hydrogel for High-Efficiency Solar Steam Generation Under 1 sun Illumination. *ACS Appl. Mater. Interfaces* **10**, 10998–11007 (2018).
109. Wakil Shahzad, M., Burhan, M., Soo Son, H., Jin Oh, S. & Choon Ng, K. Desalination processes evaluation at common platform: A universal performance ratio (UPR) method. *Appl. Therm. Eng.* **134**, 62–67 (2018).
110. Altmann, T., Robert, J., Bouma, A., Swaminathan, J. & Lienhard, J. H. Primary energy and exergy of desalination technologies in a power-water cogeneration scheme. *Appl. Energy* **252**, 113319 (2019).
111. Bouma, A. T., Swaminathan, J. & Lienhard, J. H. V. Metrics Matter: Accurately Defining Energy Efficiency in Desalination. *J. Heat Transfer* **142**, (2020).
112. Younos, T. The Economics of Desalination. *CONTEMPORARY WATER RESEARCH EDUCATION* **39**, 45 (2005).
113. Ziolkowska, J. R. Is Desalination Affordable?—Regional Cost and Price Analysis. *Water Resour. Manag.* **29**, 1385–1397 (2015).
114. Elshurafa, A. M., Albardi, S. R., Bigerna, S. & Bollino, C. A. Estimating the learning curve of solar PV balance-of-system for over 20 countries: Implications and policy recommendations. *J. Clean. Prod.* **196**, 122–134 (2018).

Acknowledgements

R.W. would like to acknowledge the funding from the Chinese Government Scholarship. W.H. would like to acknowledge the support of the Royal Academy of Engineering (RAEng) Engineering for Development Research Fellowship [grant number RF\201819\18\89] and UKRI-EPSCRC [grant number EP/W027372/1].

Author contributions

Ruoqing Wang: writing—review and editing, investigation, conceptualization, writing—original draft, data gathering, formal analysis, visualization. Wei He: conceptualization, supervision, funding acquisition, writing—review and editing.

Competing interests

The authors declare no competing interests.

Additional information

Supplementary information The online version contains supplementary material available at <https://doi.org/10.1038/s43246-024-00646-6>.

Correspondence and requests for materials should be addressed to Wei He.

Peer review information *Communications Materials* thanks Eduardo Sáez and the other anonymous reviewer for their contribution to the peer review of this work. A peer review file is available. Primary Handling Editors: John Plummer.

Reprints and permissions information is available at <http://www.nature.com/reprints>

Publisher's note Springer Nature remains neutral with regard to jurisdictional claims in published maps and institutional affiliations.

Open Access This article is licensed under a Creative Commons Attribution 4.0 International License, which permits use, sharing, adaptation, distribution and reproduction in any medium or format, as long as you give appropriate credit to the original author(s) and the source, provide a link to the Creative Commons licence, and indicate if changes were made. The images or other third party material in this article are included in the article's Creative Commons licence, unless indicated otherwise in a credit line to the material. If material is not included in the article's Creative Commons licence and your intended use is not permitted by statutory regulation or exceeds the permitted use, you will need to obtain permission directly from the copyright holder. To view a copy of this licence, visit <http://creativecommons.org/licenses/by/4.0/>.

© The Author(s) 2024